Fundamental Research 3 (2023) 967–973

Contents lists available at ScienceDirect

Fundamental Research

journal homepage: http://www.keaipublishing.com/en/journals/fundamental-research/

Article

Static analysis of elastic cable structures under mechanical load using discrete catenary theory

Weicheng Huang [a,b], Dongze He [a,b], Dezhong Tong [c], Yuzhen Chen [c,*], Xiaonan Huang [d,*], Longhui Qin [a,*], Qingguo Fei [a,b,*]

[a] School of Mechanical Engineering, Southeast University, Nanjing 211189, China
[b] Jiangsu Engineering Research Center of Aerospace Machinery, Southeast University, Nanjing 211189, China
[c] Department of Mechanical and Aerospace Engineering, University of California, Los Angeles, CA 90095, USA
[d] Department of Mechanical Engineering and Materials Science, Yale University, New Haven, CT 06511, USA

ARTICLE INFO

Article history:
Received 12 December 2021
Received in revised form 21 March 2022
Accepted 23 March 2022
Available online 31 March 2022

Keywords:
Cable structures
Rigidity
Solid mechanics
Computational mechanics
Numerical simulation
Nonlinearity

ABSTRACT

In this paper, the nonlinear mechanical response of elastic cable structures under mechanical load is studied based on the discrete catenary theory. A cable net is discretized into multiple nodes and edges in our numerical approach, which is followed by an analytical formulation of the elastic energy and the associated Hessian matrix to realize the dynamic simulation. A fully implicit framework is proposed based on the discrete differential geometry (DDG) theory. The equilibrium configuration of a target object is derived by adding damping force into the system, known as the dynamic relaxation method. The mechanical response of a single suspended cable is investigated and compared with the analytical solution for cross-validation. A more intricate scenario is further discussed in detail, where a structure consisting of multiple slender cables is connected through joints. Utilizing the robustness and efficiency of our discrete numerical framework, a systematic parameter sweep is performed to quantify the force displacement relationships of nets with the different number of cables and different directions of fibers. Finally, an empirical scaling law is provided to account for the rigidity of elastic cable net in terms of its geometric properties, material characteristics, component numbers, and cable orientations. Our results would provide new insight in revealing the connections between flexible structures and tensegrity structures, and could motivate innovative designs in both mechanical and civil engineered equipment.

1. Introduction

As a type of highly flexible one-dimensional (1D) object, elastic cables could provide an efficient and economical alternative for structures that cover a large space or span a long distance, such as cable-stay bridges and suspension roofs [1]. Recent advancements in aeronautics and astronautics further address the requirement for a general mechanical analysis on this type of highly flexible net-like objects, e.g., space debris capture with tether-net as a containment [2,3]. The cable net can also be used as a major structural component of mesh reflector deployable antennas [4].

The mathematical treatment of cable structures can date back to the 17th century when the catenary problem appeared in finding the equilibrium configuration of a flexible cable under its weight. In 1638, Galileo Galilei found that a chord under self-weight failed to maintain its originally rectilinear pattern unless some tension was applied at its boundary points [5]. Then, in 1669, Joachim Jungius noticed that the shape of a suspended chord was non-parabolic, while the exact mathematical expression of the curve could not be found. It was later solved by Christiaan Huygens through a purely geometric method and by Johann Bernoulli via an integral calculus, separately [6–8], who, however, ignored the extensibility and stretchability of elastic cables. Following Hooke's law, Leonhard Paul Euler and Daniel Bernoulli developed a variational approach to formulate the governing differential equations for a deformed cable system [9].

Although the analytical solutions for elastic catenary are available and well-known [10], numerical methods would be preferred as a more efficient tool, especially when a complex system that comprised multiple joints-connected cables was considered. Moreover, as highly geometrically nonlinear behaviors usually occur in this type of slender system, the effects of flexibility and large deflections in cable and its network should be taken into account during the establishment of equilibrium equations [11,12], which addresses the need for a numerical approach. Plenty of prior works could be found on the numerical simulation of elastic cable structures. A general two-dimensional (2D) nonlinear bar element was proposed by Kwan to provide a geometric nonlinear anal-

* Corresponding authors.
E-mail addresses: yuzhenchen@ucla.edu (Y. Chen), xiaonan.huang@yale.edu (X. Huang), lhqin@seu.edu.cn (L. Qin), qgfei@seu.edu.cn (Q. Fei).

https://doi.org/10.1016/j.fmre.2022.03.011

ysis of cable structures [11]; Abad et al. developed a new type of three-dimensional (3D) element to investigate the cable structures under general loadings [13]; Thai et al. started from a traditional elastic catenary theory and applied the incremental iterative-based method to numerically explore the nonlinear dynamics of cables [12]. Moving forward, the linear elastic property of cable structures was extended to nonlinear elasto-plastic and hyperelastic models by Chisalita and Valiente, respectively [14,15]. Both geometric and material nonlinearities were taken into account by Gobat et al. to evaluate the nonlinear mechanical response of a moving cable structure in a fluid environment [16]. For the inverse design problem, Shimoda et al. adopted an optimization-based framework to program the form-finding process of cable net structures [17].

In this century, another type of discrete framework, DDG-based formulation [18], has been widely employed in computer graphics communities to simulate the dynamics of thin elastic bodies, e.g., fur and cloth, due to its robustness and efficiency in handling the involved nonlinearity, collision, and frictional contact. In the DDG-based approach, a smooth mechanical system is discretized into multiple nodes and edges, based on which the nonlinear elastic potentials are formulated. Previous DDG-based methods have shown surprising success in simulating the thin elastic structures, e.g. 1D rod [19–22], 2D plate/shell [23–25], an intermediate form between 1D slender rod and 2D thin plate – named as ribbon [26,27], and hollow gridshell [28–33]. However, almost all of those DDG-based simulations focused on the bending-dominated deformations of thin elastic bodies. Elastic cable structure, on the other side, can only undergo pure stretching as its transverse bending rigidity is assumed to be zero, which differs from the classical beam or rod model that encompasses multiple modes, e.g., stretching, bending, and twisting [19,20]. From a mathematical point of view, when a 1D object is with length L, stretching stiffness EA, bending stiffness EI, and under an external load F, a beam model would be effective if $EA \gg F \sim EI/L^2$, while a cable model should be considered in the case $EA \sim F \gg EI/L^2$. Whereas, when the intermediate circumstance appears, i.e., $EA \gg F \gg EI/L^2$, the configuration of a 1D structure is merely governed by its geometric characteristics and boundary conditions, and the problem becomes material-independent, e.g., an inextensible catenary under its self-weight.

In the current numerical investigation, we focus on the high tension range, $EA \sim F \gg EI/L^2$, and leverage a discrete catenary theory to numerically evaluate the force displacement relation of elastic cable structures under mechanical loads. A continuous cable structure is discretized into multiple nodes connected by edges, based on which the elastic stretching potential and its Hessian matrix are evaluated explicitly through the DDG approach. Here, as the absolute nodal coordinate formulation is used within our numerical framework, the geometrically nonlinear deformations of cable structures can be captured automatically, e.g., large deflections and large rotations. Moreover, compared with previous methods [34–36], this type of discrete node-based formulation could capture more general loading conditions, such as dynamic loadings, and made it easier to handle contact, friction, collision, and fluid-structure interaction, which are necessary for real engineering use, e.g., dynamic simulation of soft robots [37,38] and capture of space debris [2,3]. The nonlinear dynamics of a cable net is later solved by integrating the discrete equations of motion step by step. Its final equilibrium configuration is obtained with the damping force added into the dynamic system. The mechanics of a single catenary is analyzed, followed by the discussion on the mechanical performances of a cable net structure. It is found that the relative rigidity of a cable network would linearly augment as the number of cables increases. The dependence of structural rigidity on the fiber orientation can be described with a Cosine-like function. Finally, an empirical scaling law is provided to non-dimensionally describe the force displacement relation of a cable net with different cable numbers and different fiber orientations. In parallel with extensive numerical explorations, the analytical solutions for a single cable system under mechanical loads are formulated for cross-validation.

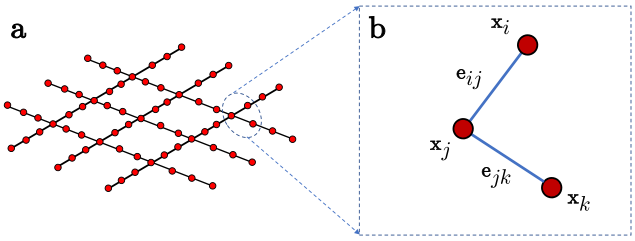

Fig. 1. Discrete model. (a) Discrete diagram of an elastic cable structure. (b) Notations used in our numerical simulation.

This paper mainly contributes in the following aspects: (1) A fully implicit numerical framework for the simulation of cable structures is derived based on DDG. (2) The analytical solution for a single cable system is formulated to validate our newly-introduced simulator. (3) The geometrically nonlinear mechanics of a squared cable net is explored numerically through our discrete model.

The remaining paper is organized as follows. In Section 2, the discrete catenary method for the simulation of elastic cable structures under mechanical loads is introduced, followed by a description of single cable structures and cable nets in Section 3. What's more, the analytical solution for the mechanical response of a single cable system is derived in parallel for the validation of our newly-introduced numerical framework. Finally, conclusive remarks and future research directions are discussed in Section 4.

2. Discrete numerical method

In this section, we introduce a discrete model for the numerical simulation of elastic nets under mechanical loads. The cable structure considered here is assumed to be manufactured by an isotropic, linearly elastic material with Young's modulus E, Poisson's ratio ν, and circular cross-section with radius r_0 (and, therefore, cross-sectional area $A = \pi r_0^2$). Referring to Fig. 1a, a group of elastic cables is connected by multiple joints, and the whole structure is discretized into N nodes, resulting in a $3N$ sized degrees of freedom (DOF) vector:

$$\mathbf{q} \equiv [\mathbf{x}_0, \mathbf{x}_1, \dots, \mathbf{x}_i, \dots, \mathbf{x}_{N-1}]^T, \text{ with } i \in [0, N-1] \tag{1}$$

The edge vector between the ith and the jth node is denoted by:

$$\mathbf{e}^{ij} = \mathbf{x}_i - \mathbf{x}_j \tag{2}$$

as details can be found in Fig. 1b. To follow the convention of discrete model, the subscripts are adopted for the quantities associated with nodes, and the superscripts are adopted for the quantities associated with edges. As the elastic cable can only experience uniaxial stretching, and the bending and twisting of cable centerline are forbidden, the elastic potential of a cable net structure is given by

$$E_{\text{elastic}} = \sum_{ij}^{N_{\text{edge}}} \frac{1}{2} EA\left(\epsilon^{ij}\right)^2 |\bar{\mathbf{e}}^{ij}| \tag{3}$$

where EA is the stretching stiffness, N_{edge} is the total discrete edge number, and the stretching strain of the (ij)th edge is

$$\epsilon^{ij} = \frac{|\mathbf{e}^{ij}|}{|\bar{\mathbf{e}}^{ij}|} - 1 \tag{4}$$

Here, a bar on the top represents the quantities in an undeformed configuration, e.g., $\bar{\mathbf{e}}^{ij}$ is the undeformed length of the (ij)th edge. The Hessian matrix (also known as tangential stiffness matrix) is the second variation of total potentials:

$$\mathbb{K} = \frac{\partial^2 E_{\text{elastic}}}{\partial \mathbf{q}^2} \tag{5}$$

Specifically, the Hessian associated with the (ij)th edge is

$$\frac{\partial^2 E_{\text{elastic}}}{\partial \mathbf{e}^{ij} \partial \mathbf{e}^{ij}} = \frac{\partial^2 E_{\text{elastic}}}{\partial^2 \epsilon^{ij}} \frac{\partial \epsilon^{ij}}{\partial \mathbf{e}^{ij}} \otimes \frac{\partial \epsilon^{ij}}{\partial \mathbf{e}^{ij}} + \frac{\partial E_{\text{elastic}}}{\partial \epsilon^{ij}} \frac{\partial^2 \epsilon^{ij}}{\partial \mathbf{e}^{ij} \partial \mathbf{e}^{ij}} \tag{6}$$

where $\otimes$ is the tensor product. The formulations of material-related terms are straightforward, i.e.

$$\begin{aligned}\frac{\partial E_{\text{elastic}}}{\partial \epsilon^{ij}} &= EA\epsilon^{ij}|\bar{\mathbf{e}}^{ij}| \\ \frac{\partial^2 E_{\text{elastic}}}{\partial^2 \epsilon^{ij}} &= EA|\bar{\mathbf{e}}^{ij}|\end{aligned} \tag{7}$$

while the geometry-related terms are procured on the basis of differential geometry [22]:

$$\begin{aligned}\frac{\partial \epsilon^{ij}}{\partial \mathbf{e}^{ij}} &= \frac{1}{|\bar{\mathbf{e}}^{ij}|}\mathbf{t}^{ij} \\ \frac{\partial^2 \epsilon^{ij}}{\partial \mathbf{e}^{ij}\partial \mathbf{e}^{ij}} &= \frac{1}{|\bar{\mathbf{e}}^{ij}|}\frac{(\mathbb{I}_3 - \mathbf{t}^{ij}\otimes\mathbf{t}^{ij})}{|\mathbf{e}^{ij}|}\end{aligned} \tag{8}$$

where $\mathbb{I}_3$ is a 3×3 identity matrix and $\mathbf{t}^{ij} = \mathbf{e}^{ij}/|\mathbf{e}^{ij}|$ is the tangential direction of (ij)th edge. Finally, the Hessian with respect to DOF vector, $\mathbf{x}_i$, can be easily obtained based on the chain rule acquired in Eq. 2.

The equations of motion for a dynamic cable net system is given by Huang and Jawed [39]:

$$\mathbb{M}\ddot{\mathbf{q}} + \mathbb{C}\dot{\mathbf{q}} + \mathbb{K}\mathbf{q} - \mathbf{F}^{\text{ext}} = \mathbf{0} \tag{9}$$

where $\mathbb{M}$ is the diagonal mass matrix, $\mathbb{C}$ is the damping matrix, and $\mathbf{F}^{\text{ext}}$ is the external force. Here, the damping matrix is determined by the damping coefficient, μ. It is known that the damping coefficient is rather important for the decay rate, while has no contribution to the final static configuration. Here, the damping coefficient is set to be $\mu = 1.0$. Details can be found in Appendix A. Euler method is used to update the DOF vector $\mathbf{q}$ and its velocity (time derivative of DOF) $\mathbf{v} = \dot{\mathbf{q}}$ from time step t_k to $t_{k+1} = t_k + h$ (here h is the time step size):

$$\mathbf{E} \equiv \mathbb{M}\left(\frac{\mathbf{q}_{k+1} - \mathbf{q}_k}{h^2} - \frac{\mathbf{v}_k}{h}\right) + \mathbb{C}\mathbf{v}_{k+1} + \mathbb{K}\mathbf{q}_{k+1} - \mathbf{F}^{\text{ext}}_{k+1} = \mathbf{0} \tag{10a}$$

$$\mathbf{q}_{k+1} = \mathbf{q}_k + \Delta\mathbf{q}_{k+1} \tag{10b}$$

$$\mathbf{v}_{k+1} = \frac{1}{h}\Delta\mathbf{q}_{k+1} \tag{10c}$$

The Newton-Raphson method is applied to solve this set of nonlinear equations of motion. At each time step t_{k+1}, a new solution is first guessed on the basis of the previous state, i.e.

$$\mathbf{q}^0_{k+1} = \mathbf{q}_k + h\mathbf{v}_k \tag{11}$$

Then, the solutions are optimized by gradient decent algorithm, such that the new solution at the $(m+1)$th step is

$$\mathbf{q}^{m+1}_{k+1} = \mathbf{q}^m_{k+1} - \mathbb{J}^m \backslash \mathbf{E}^m \tag{12}$$

where $\mathbb{J}$ is the Jacobian matrix associated with Eq. 10:

$$\mathbb{J} = \frac{\mathbb{M}}{h^2} + \frac{\mathbb{C}}{h} + \mathbb{K} \tag{13}$$

Here, the Jacobian associated with the external actuation forces is zeros. The equations of motion is updated iteratively until the error in the current time step decreases within the prescribed tolerance. Moreover, with damping forces added into the dynamic system, the equilibrium configurations of elastic structures can be eventually derived through a so-called dynamic relaxation method. The overall computational time are provided in Appendix B.

3. Results

In this section, a systematic investigation of the mechanical responses of elastic cable structures is presented in detail. A simple single cable system is analyzed firstly, and a more complex net-like object comprised of multiple slender fibers is then discussed. In addition, the analytical solution of a single cable structure under mechanical loads is derived for comparison.

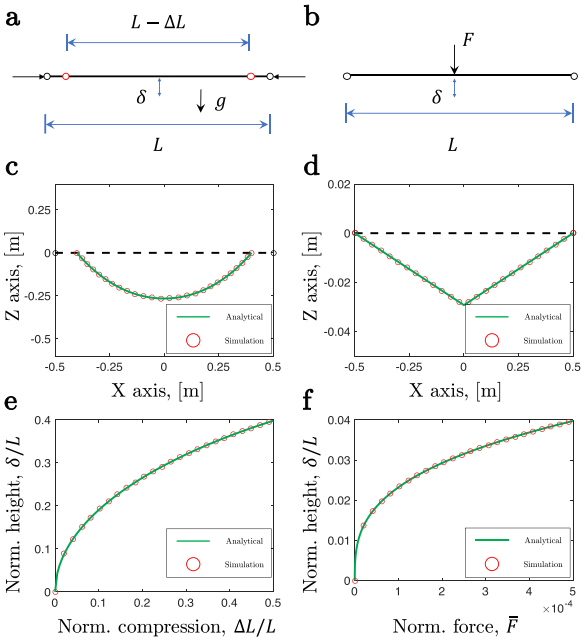

Fig. 2. Numerical investigations of a single cable structure. The boundary conditions and load conditions for (a) a suspended catenary and (b) a pin-pin cable under midpoint actuation. Undeformed and deformed configurations of (c) an inextensible catenary and (d) a stretchable cable. Normalized midpoint displacement, δ/L, as a function of (e) normalized uniaxial compression, $\Delta L/L$, and (f) normalized external force, $\bar{F}$.

3.1. Mechanics of single cable structure

Herein, two cases of a single cable system are considered. The elastic cable is of length $L = 1.0$ m, cross-section radius $r_0 = 1.0$ cm, and Young's modulus $E = 10$MPa. The effect of Poisson's ratio is negligible as the structure studied here can only experience uniaxial stretching. To achieve a pin-pin-like boundary condition, the first node, $\mathbf{x}_0$, as well as the last node, $\mathbf{x}_{N-1}$, are fixed or constrained along a prescribed path. All other nodes are free to evolve based on the statement of force balance. The number of vertexes is selected as $N = 100$ after a convergence study. As only equilibrium configuration is focused, the dynamic parameters (such as time step size and damping coefficient) are randomly chosen for convenience.

In Fig. 2a, the topology of a suspended cable under gravity is presented. The gravitational potential is assumed to be much smaller compared with the elastic stretching energy, $\rho ALg \ll EA$, i.e., the cable is inextensible and the influence of gravity is trivial so that the analytical solution is obtainable. When the boundary distance is shrunk from L to $L - \Delta L$, the pattern of a suspended cable is a catenary:

$$\begin{aligned}z(x) &= A\cosh(\tfrac{x}{A}) - A\cosh(\tfrac{L-\Delta L}{2A}) \\ &\text{with } x \in [-\tfrac{L-\Delta L}{2}, \tfrac{L-\Delta L}{2}]\end{aligned} \tag{14}$$

where the coefficient A can be derived by solving the following transcendental equation:

$$2A\sinh(\frac{L-\Delta L}{2A}) = L \tag{15}$$

In Fig. 2c, the deformed configuration of a suspended catenary is shown when $\Delta L/L = 0.2$ from both numerical simulation (symbols) and analytical approach (solid lines). The dependence of normalized structural maximum deflection, δ/L, on its normalized compressive displacement, $\Delta L/L$, is plotted in Fig. 2e. Quantitative agreement between the numerical simulation and the analytical solution indicates the accuracy of our DDG-based model.

A stretchable cable under midpoint load is given in Fig. 2b. In contrast to the well-known simply-supported beam that can bear a bending-

type deformation, the cable structure can only experience pure stretching, and, as a result, a zigzag line is observed when a structure is loaded onto its midpoint, referring to Fig. 2d. The deformed pattern is a piecewise linear function:

$$z(x) = \begin{cases} -2\frac{\delta}{L}x - \delta \text{ when } x \in [-\frac{L}{2}, 0] \\ 2\frac{\delta}{L}x - \delta \text{ when } x \in [0, \frac{L}{2}] \end{cases} \tag{16}$$

where the midpoint displacement δ is obtained by solving the following equilibrium equation,

$$F = 2EA\left[\frac{\sqrt{\delta^2 + (L/2)^2} - L/2}{L/2}\right]\frac{\delta}{\sqrt{\delta^2 + (L/2)^2}} \tag{17}$$

The deformed configurations and the force displacement curves from both numerical solution (symbols) and analytical formulation (solid lines) can be found in Fig. 2d and f, respectively. Here, the maximum uniaxial stretching strain is within 5% to ensure the effectiveness of the linear elasticity. It should be noted that the force is normalized by $\bar{F} = F/EA$.

3.2. Mechanics of cable net structure

Moving forward, a more complex object consisting of multiple connected cables is considered. Referring to Fig. 3, the geometric parameters of our cable net are: $L \times L = 1\ \text{m} \times 1\ \text{m}$, fiber orientation, $\alpha \in [0, \pi/2]$, and total cable number $n \in [10, 34]$. Young's modulus is $E = 10$ MPa, which is identical to the previous single cable scenario. The external distributed load is denoted as p and the midpoint displacement is measured by δ. In our numerical framework, the discrete external force is applied on the z-DOF of each node and its magnitude is pL^2/N, where N is the total nodal number. Similar to the previous case, a pin-pin boundary condition is achieved by fixing two boundary nodes of each cable (red dots in Fig. 3). As the length of each cable would be different from each other, the discrete edge length $|\bar{\mathbf{e}}^{ij}| = 1$cm is adopted after a convergence study. In Fig. 4, the deformed configurations of elastic

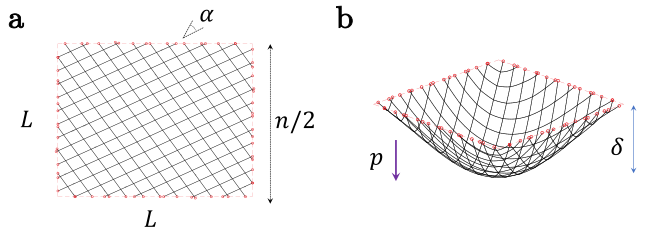

Fig. 3. Diagrams of cable net. Schematic diagram of an elastic cable net in its (a) undeformed configuration and (b) deformed pattern. Here, the cable net is in size of $L \times L$, wih cable number n, cable orientation α, distributed load p, and its midpoint displacement is δ.

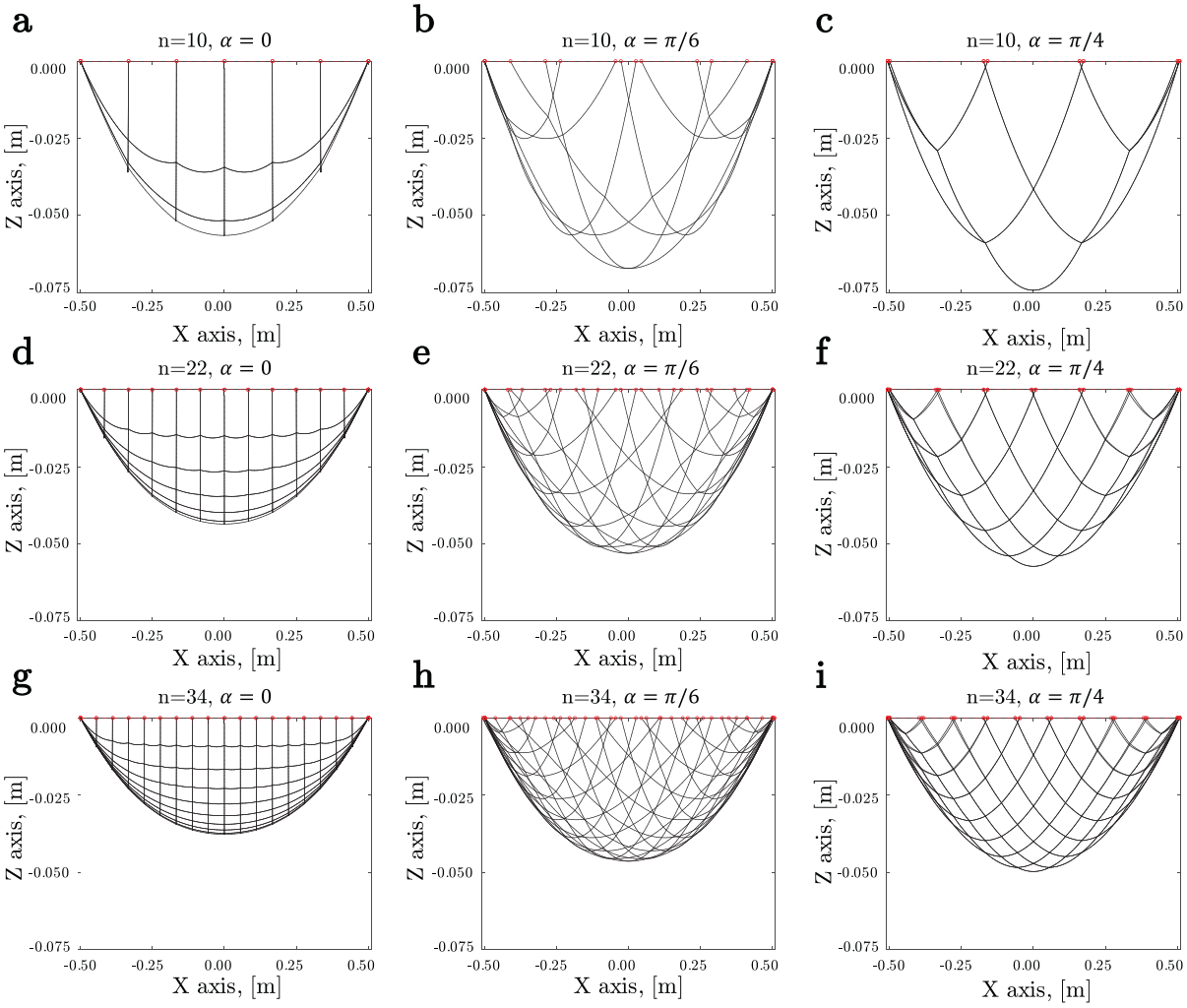

Fig. 4. Deformed configurations of cable nets. The configurations of elastic nets with different numbers of cables and different orientations of fibers. (a) $n = 10$, $\alpha = 0$; (b) $n = 10$, $\alpha = \pi/6$; (c) $n = 10$, $\alpha = \pi/4$; (d) $n = 22$, $\alpha = 0$; (e) $n = 22$, $\alpha = \pi/6$; (f) $n = 22$, $\alpha = \pi/4$; (g) $n = 34$, $\alpha = 0$; (h) $n = 34$, $\alpha = \pi/6$; (i) $n = 34$, $\alpha = \pi/4$.

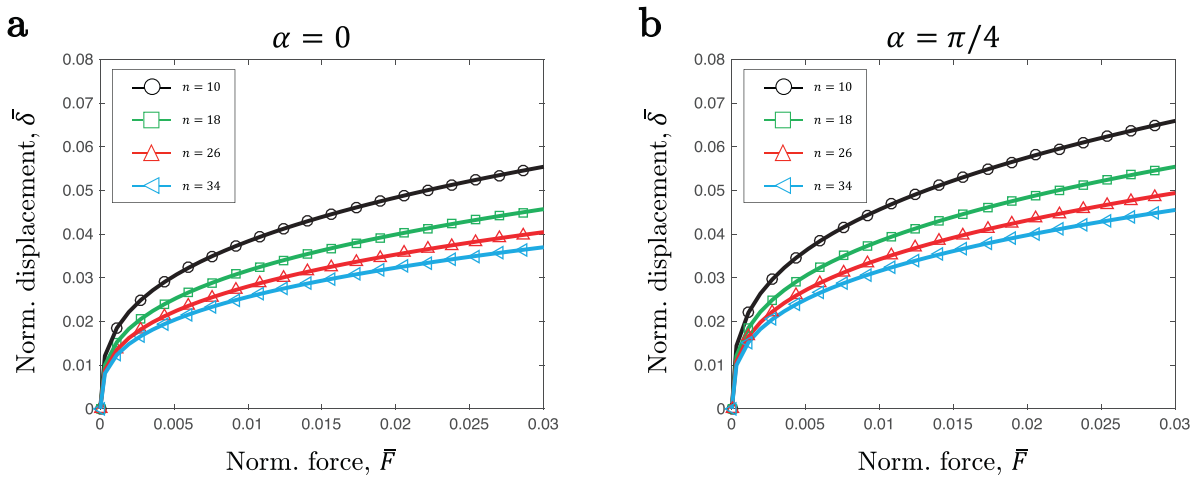

Fig. 5. Force-displacement curves for cable nets. Normalized force displacement curves of elastic nets with different numbers of cables, $n \in \{10, 18, 26, 34\}$. Here, the rotational angle is constrained as (a) $\alpha = 0.0$ and (b) $\alpha = \pi/4$.

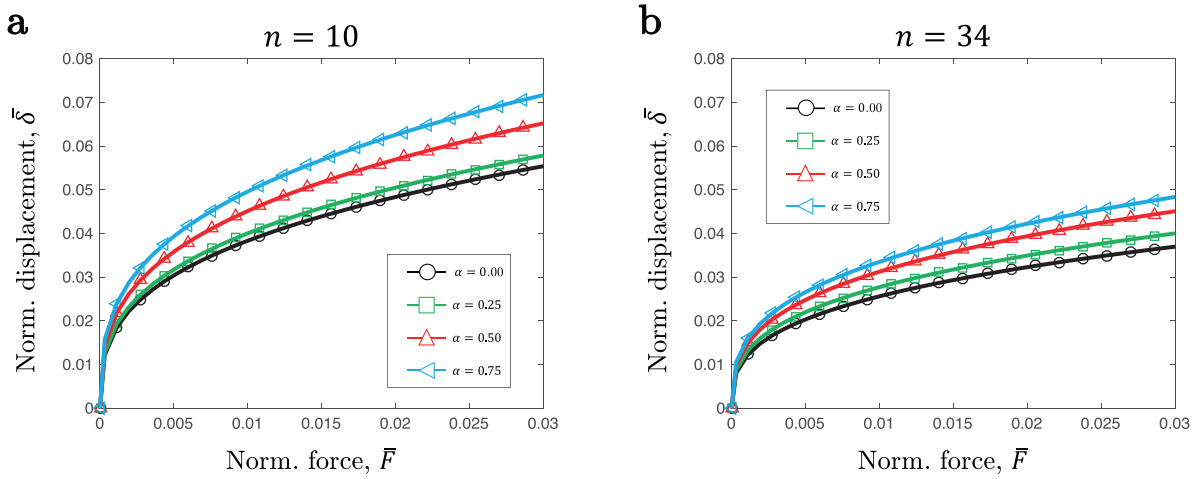

Fig. 6. Force-displacement curves for cable nets. Normalized force displacement curves of elastic nets with different rotational angles, $\alpha \in \{0.00, 0.25, 0.50, 0.75\}$. Here, the total cable number is fixed as (a) $n = 10$ and (b) $n = 34$.

cable nets with different fiber numbers and fiber orientations are presented. Here, the distributed load is $p = 100$Pa (resulting $\bar{F} = pL^2/EA \approx 0.032$). It should be noted that in contrast to the global deformed configuration of bending-dominated gridshells [28,29,31–33], the elastic cable nets would deform locally, i.e., the catenary-like pattern is observed between two consecutive joints.

For a quantitative understanding of the mechanics of cable nets under mechanical loads, we first consider the influence of cable number on its force displacement curves. In Fig. 5a, b, the rotational angle is fixed as $\alpha = 0$ and $\alpha = \pi/4$, separately, and the force displacement curves are plotted with respect to different cable numbers $n \in \{10, 18, 26, 34\}$. As expected, the rigidity of cable nets is enhanced with the increase of cable numbers. To quantitatively reveal the dependence of structural rigidity on its component number, Fig. 7a gives the normalized displacement, δ/L, as a function of total cable number n, with a fixed external load, $p = 10$ Pa ($\bar{F} \approx 0.0032$). The maximum displacement almost linearly decreases when the cable number becomes larger.

The effect of fiber orientation is further considered. In Fig. 6, the normalized force displacement curves of elastic cable nets are presented with different rotational angles, $\alpha \in \{0.00, 0.25, 0.50, 0.75\}$. The cable number is fixed as $n = 10$ in Fig. 6a and $n = 34$ in Fig. 6b. Moreover, the variation of normalized midpoint displacement, δ/L, on rotational angle, α, is presented in Fig. 7b. It is found that the relative deflection of the cable net follows a trigonometric (Sine/Cosine) trend when the cable orientation changes from 0 to $\pi/2$.

After a systematical exploration of the relevant parameters of cable nets, an empirical scaling law is provided to describe the dimensionless mechanics of cable nets. Specifically, a nondimensional force-displacement relationship is focused. According to Buckingham-pi theorem, the normalized displacement, $\bar{\delta} = \delta/L$, only depends on three nondimensional groups: normalized distributed load, $\bar{F} = pL^2/EA$, number of cables, n, and fiber orientations, α. It is indicated by our numerical findings that the force-displacement relationship of a squared cable net under distributed load can be well described by

$$\bar{\delta}/f(\alpha) \sim \bar{F}/n \tag{18}$$

where the denominator on the left side is a trigonometric function:

$$f(\alpha) = \frac{(D-1)}{2}\cos(4\alpha + \pi) + \frac{(D+1)}{2} \tag{19}$$

Herein, the coefficient D is approximate 1.31 after an empirical data fitting. Remarkably, the scaling law in Eq. 18 can capture all the data generated by our well-established numerical framework, as shown in Fig. 8.

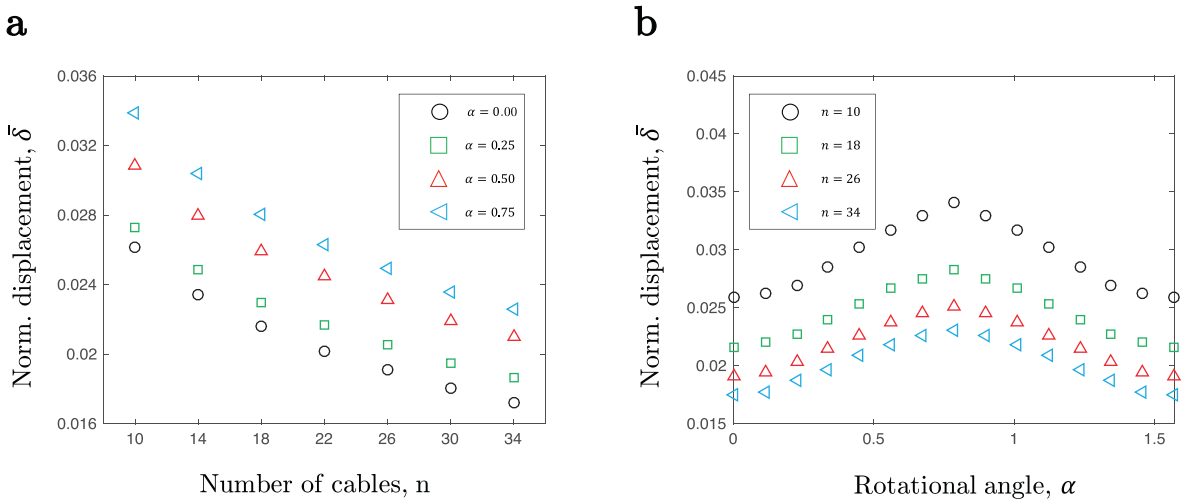

Fig. 7. Variations of geometric parameters. Normalized midpoint displacement, $\bar{\delta} = \delta/L$, as a function of (a) cable number n and (b) rotational angle α. Here, the external distributed load is selected as $p = 10$ Pa, resulting $\bar{F} = pL^2/EA \approx 0.0032$.

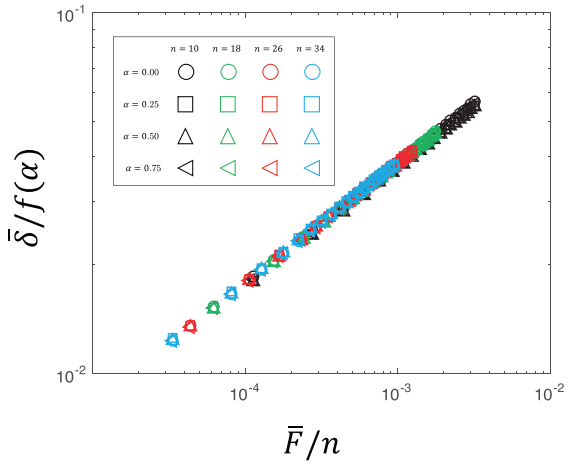

Fig. 8. Scaling law. Scaling law between $\bar{\delta}/f(\alpha)$ and $\bar{F}/n$.

4. Conclusion

In this paper, the mechanical response of cable nets was investigated through a discrete catenary-based approach. A DDG-based numerical framework was employed to capture the geometrically nonlinear dynamics of 1D network, and its equilibrium configuration was derived by utilizing the dynamic relaxation method. In addition to the extensive numerical explorations, the solutions for a single cable system were procured analytically for cross-validation. Quantitative agreements between the numerical simulations and the analytical results indicated the accuracy of our DDG-based formulation. Similar to the bending-dominated elastic gridshells, it was found that the relative rigidity of stretching-dominated cable nets was linearly enhanced as the structures became denser. Moreover, the relevance between the structural rigidity and the fiber orientation can be accurately described by a Cosine-like function. Finally, a robust scaling law was proposed empirically to provide a nondimensional force-displacement relation of the catenary nets with respect to different cable numbers and fiber orientations. It should be noted that the current numerical investigation is limited within a small stretching strain regime, e.g., $\epsilon \sim 5\%$. In the case that the uniaxial stretching strain of cable nets is no longer small, e.g., $\epsilon \gg 10\%$, the naive linear elastic model needs to be replaced by the nonlinear hyperelastic theory, which can capture the material nonlinearity. Next, more attentions should be paid to the contact-based numerical framework of net structures, which is critical for the dynamic simulation of space debris capture and removal.

Declaration of competing interest

The authors declare that they have no conflicts of interest in this work.

Acknowledgments

This work was supported by the National Natural Science Foundation of China (52125209) and Fundamental Research Funds for the Central Universities (2242021R10024).

Appendix A. Effect of damping coefficient

In this section, we discuss the damping coefficient formulated in $\mathbb{C}$. In Fig. A9, we plot the midpoint deflection as a function of time for a cable structure with $n = 10$ and $\alpha = 0.0$, which is identical to Fig. 4a. Even though the dynamic process would be different for different damping coefficients μ, the final equilibrium configurations are uniform regardless of μ.

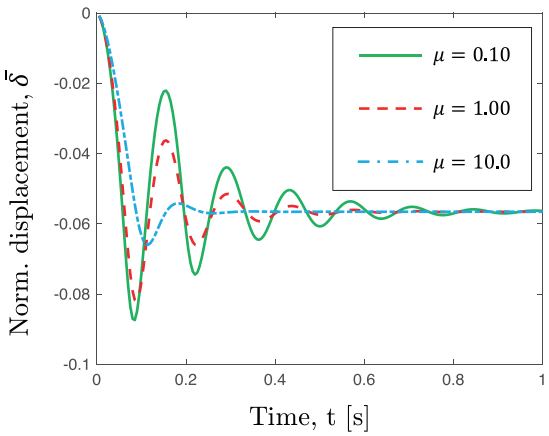

Fig. A.9. Dynamic simulations. The midpoint displacement as a function of time for different damping coefficient $\mu \in \{0.10, 1.00, 10.0\}$. Here, a cable net with $n = 10$ and $\alpha = 0.0$ is considered.

Appendix B. Computational time

In this appendix, we focus on the computational efficiency of our discrete approach. In Fig. B10, we found that the computational time linearly scales with the time step size h. The final results can be derived within 20s even for a relatively dense net (with $n = 34$ and total DOF number ~ 13000). The simulations are performed on a single thread of Intel Core i7-6600U Processor @3.4GHz. PARDISO is used when solving a sparse linear system in our numerical experiments [40–42].

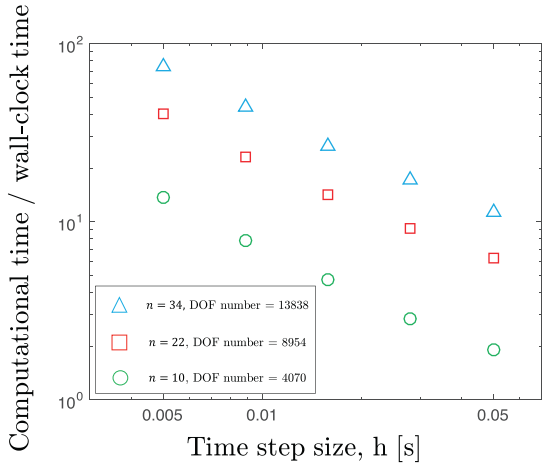

Fig. B.10. Computational time. The ratio between computational time and wall-clock time as a function of time step size h in different scenarios, $n \in \{10, 22, 34\}$.

References

[1] H. Jayaraman, W. Knudson, A curved element for the analysis of cable structures, Comput. Struct. 14 (3–4) (1981) 325–333.
[2] E.M. Botta, I. Sharf, A.K. Misra, et al., On the simulation of tether-nets for space debris capture with vortex dynamics, Acta Astronaut. 123 (2016) 91–102.
[3] E.M. Botta, I. Sharf, A.K. Misra, Contact dynamics modeling and simulation of tether nets for space-debris capture, J. Guid. Control Dyn. 40 (1) (2017) 110–123.
[4] Y. Zhang, N. Li, G. Yang, et al., Dynamic analysis of the deployment for mesh reflector deployable antennas with the cable-net structure, Acta Astronaut. 131 (2017) 182–189.
[5] G. Galilei, Discorsi e dimostrazioni matematiche, intorno à due nuoue fcienze, vol. 1, Publicacions de la Universitat Autònoma de Barcelona, 1988.
[6] J. Bernoulli, Solutions to the problem of the catenary, or funicular curve, Acta Eruditorum 1691 (2001).
[7] J. Bernoulli, W. Ferguson, Lectures on the integral calculus, 21ST Century Sci. Technol. 17 (1) (2004) 34–42.
[8] G. Leibniz, The string whose curve is described as bending under its own weight, and the remarkable resources that can be discovered from it by however many proportional means and logarithms, Acta Eruditorum 1691 (2001).
[9] C.G. Fraser, Leonhard Euler, Book on the calculus of variations (1744), in: Landmark Writings in Western Mathematics 1640–1940, Elsevier, 2005, pp. 168–180.
[10] T. O'Brien, General solution of suspended cable problems, J. Struct. Div. 93 (1) (1967) 1–26.
[11] A. Kwan, A new approach to geometric nonlinearity of cable structures, Comput. Struct. 67 (4) (1998) 243–252.
[12] H.-T. Thai, S.-E. Kim, Nonlinear static and dynamic analysis of cable structures, Finite Elem. Anal. Des. 47 (3) (2011) 237–246.
[13] Y. Yang, J.-Y. Tsay, Geometric nonlinear analysis of cable structures with a two-node cable element by generalized displacement control method, Int. J. Struct. Stab. Dyn. 7 (04) (2007) 571–588.
[14] A. Chisalita, Finite deformation analysis of cable networks, J. Eng. Mech. 110 (2) (1984) 207–223.
[15] A. Valiente, Symmetric catenary of a uniform elastic cable of neo-Hookean material, J. Eng. Mech. 132 (7) (2006) 747–753.
[16] J. Gobat, M. Grosenbaugh, Time-domain numerical simulation of ocean cable structures, Ocean Eng. 33 (10) (2006) 1373–1400.
[17] M. Shimoda, K. Yamane, J.-X. Shi, Non-parametric shape optimization method for designing cable net structures in form finding and stiffness maximization problems, Int. J. Solids Struct. 146 (2018) 167–179.
[18] E. Grinspun, M. Desbrun, K. Polthier, et al., Discrete differential geometry: an applied introduction, ACM SIGGRAPH Course 7 (2006) 1–139.
[19] M. Bergou, M. Wardetzky, S. Robinson, et al., Discrete elastic rods, in: ACM Transactions on Graphics (TOG), vol. 27, ACM, 2008, p. 63.
[20] M. Bergou, B. Audoly, E. Vouga, et al., Discrete viscous threads, in: ACM Transactions on Graphics (TOG), vol. 29, ACM, 2010, p. 116.
[21] M.K. Jawed, F. Da, J. Joo, et al., Coiling of elastic rods on rigid substrates, Proc. Natl. Acad. Sci. 111 (41) (2014) 14663–14668.
[22] M.K. Jawed, A. Novelia, O.M. O'Reilly, A Primer on the Kinematics of Discrete Elastic Rods, Springer, 2018.
[23] D. Baraff, A. Witkin, Large steps in cloth simulation, in: Proceedings of the 25th Annual Conference on Computer Graphics and Interactive Techniques, ACM, 1998, pp. 43–54.
[24] E. Grinspun, A.N. Hirani, M. Desbrun, et al., Discrete shells, in: Proceedings of the 2003 ACM SIGGRAPH/Eurographics Symposium on Computer animation, Eurographics Association, 2003, pp. 62–67.
[25] W. Huang, Y. Wang, X. Li, et al., Shear induced supercritical pitchfork bifurcation of pre-buckled bands, from narrow strips to wide plates, J. Mech. Phys. Solids 145 (2020) 104168.
[26] W. Huang, C. Ma, L. Qin, Snap-through behaviors of a pre-deformed ribbon under midpoint loadings, Int. J. Solids Struct. (2021) 111184.
[27] B. Audoly, S. Neukirch, A one-dimensional model for elastic ribbons: a little stretching makes a big difference, J. Mech. Phys. Solids 153 (2021) 104457.
[28] C. Baek, A.O. Sageman-Furnas, M.K. Jawed, et al., Form finding in elastic gridshells, Proc. Natl. Acad. Sci. 115 (1) (2018) 75–80.
[29] C. Baek, P.M. Reis, Rigidity of hemispherical elastic gridshells under point load indentation, J. Mech. Phys. Solids 124 (2019) 411–426.
[30] L. Qin, W. Huang, Y. Du, et al., Genetic algorithm-based inverse design of elastic gridshells, Struct. Multidiscip. Optim. (2020) 1–17.
[31] W. Huang, L. Qin, M. Khalid Jawed, Numerical method for direct solution to form-finding problem in convex gridshell, J. Appl. Mech. 88 (2) (2021) 021012.
[32] W. Huang, L. Qin, Q. Chen, Numerical exploration on snap buckling of a pre-stressed hemispherical gridshell, J. Appl. Mech. 89 (1) (2021) 011005.
[33] W. Huang, L. Qin, Q. Chen, Natural frequencies of pre-buckled rods and gridshells, Appl. Math. Model. (2022).
[34] K. Ahmadi-Kashani, Development of cable elements and their applications in the analysis of cable structures., University of Manchester Institute of Science and Technology (UMIST), 1983 Ph.D. thesis.
[35] K. Ahmadi-Kashani, A. Bell, The analysis of cables subject to uniformly distributed loads, Eng. Struct. 10 (3) (1988) 174–184.
[36] K. Ahmadi-Kashani, Representation of cables in space subjected to uniformly distributed loads, Int. J. Space Struct. 3 (4) (1988) 221–230.
[37] W. Huang, X. Huang, C. Majidi, et al., Dynamic simulation of articulated soft robots, Nat. Commun. 11 (1) (2020) 1–9.
[38] W. Huang, Z. Patterson, C. Majidi, et al., Modeling soft swimming robots using discrete elastic rod method, in: Bioinspired Sensing, Actuation, and Control in Underwater Soft Robotic Systems, Springer, 2021, pp. 247–259.
[39] W. Huang, M.K. Jawed, Newmark-beta method in discrete elastic rods algorithm to avoid energy dissipation, J. Appl. Mech. 86 (8) (2019).
[40] M. Bollhöfer, O. Schenk, R. Janalík, et al., State-of-the-art sparse direct solvers, arXiv preprint arXiv:1907.05309 (2019).
[41] C. Alappat, A. Basermann, A.R. Bishop, et al., A recursive algebraic coloring technique for hardware-efficient symmetric sparse matrix-vector multiplication, ACM Trans. Parallel Comput. (TOPC) 7 (3) (2020) 1–37.
[42] M. Bollhofer, A. Eftekhari, S. Scheidegger, et al., Large-scale sparse inverse covariance matrix estimation, SIAM J. Sci. Comput. 41 (1) (2019) A380–A401.

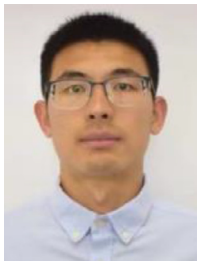

Weicheng Huang (BRID: 08701.00.00388) is an associate professor at Southeast University, China. He graduated from Tongji University and UCLA. His research interests include structural dynamics, solid mechanics, nonlinear mechanics, fluid-structure interaction, and soft robotics.

Qingguo Fei is a professor at Southeast University, China. He graduated from Nanjing University of Aeronautics and Astronautics. His research interests include structural dynamics, inverse problems as system identification, structural vibration acoustics/vibro-acoustics, dynamical strength assessment and composite material.